Model Studies of Hydrogen Atom Addition and Abstraction Processes Involving *ortho*-, *meta*-, and *para*-Benzynes

Aurora E. Clark and Ernest R. Davidson*

Contribution from the Department of Chemistry, Indiana University, Bloomington, Indiana 47405-7102

Received April 6, 2001. Revised Manuscript Received July 9, 2001

Abstract: H-atom addition and abstraction processes involving *ortho*-, *meta*-, and *para*-benzyne have been investigated by multiconfigurational self-consistent field methods. The $H_A + H_B\cdots H_C$ reaction (where r_{BC} is adjusted to mimic the appropriate singlet−triplet energy gap) is shown to effectively model H-atom addition to benzyne. The doublet multiconfiguration wave functions are shown to mix the "singlet" and "triplet" valence bond structures of $H_B\cdots H_C$ along the reaction coordinate; however, the extent of mixing is dependent on the singlet−triplet energy gap (ΔE_{ST}) of the $H_B\cdots H_C$ diradical. Early in the reaction, the ground-state wave function is essentially the "singlet" VB function, yet it gains significant "triplet" VB character along the reaction coordinate that allows H_A-H_B bond formation. Conversely, the wave function of the first excited state is predominantly the "triplet" VB configuration early in the reaction coordinate, but gains "singlet" VB character when the H-atom is close to a radical center. As a result, the potential energy surface (PES) for H-atom addition to triplet $H_B\cdots H_C$ diradical is repulsive! The H_3 model predicts, in agreement with the actual calculations on benzyne, that the singlet diradical electrons are not coupled strongly enough to give rise to an activation barrier associated with C−H bond formation. Moreover, this model predicts that the PES for H-atom addition to triplet benzyne will be characterized by a repulsive curve early in the reaction coordinate, followed by a potential avoided crossing with the $(\pi)^1(\sigma^*)^1$ state of the phenyl radical. In contrast to H-atom addition, large activation barriers characterize the abstraction process in both the singlet ground state and first triplet state. In the ground state, this barrier results from the weakly avoided crossing of the dominant VB configurations in the ground-state singlet (S_0) and first excited singlet (S_1) because of the large energy gap between S_0 and S_1 early in the reaction coordinate. Because the S_1 state is best described as the combination of the triplet X−H bond and the triplet $H_B\cdots H_C$ spin couplings, the activation barrier along the S_0 abstraction PES will have much less dependence on the ΔE_{ST} of $H_B\cdots H_C$ than previously speculated. For similar reasons, the T_1 potential surface is quite comparable to the S_0 PES.

Introduction

The ground-state singlet diradicals *ortho*-, *meta*-, and *para*-benzyne exhibit versatile chemical reactivity, ranging from electrophilic and nucleophilic reactions to radical processes that are characteristic of the phenyl radical. Gas-phase negative ion photoelectron spectroscopy and matrix isolation techniques are the primary experimental tools for probing the reactivity and electronic structure of the benzyne diradicals. Theory has also played an important role in the study of these intermediates. High-level ab initio and density functional theory (DFT) calculations accurately predict the stability of benzyne in the order *ortho* > *meta* > *para*, as well as the stabilization energies of the singlet ground states relative to the first respective vertical triplet states (ΔE_{ST}).[1−7] *ortho*-Benzyne, an important synthetic intermediate, has been well characterized both theoretically and experimentally. However, very little has been reported about the chemistry of *meta*-[1] and *para*-benzynes. Although interest in *para*-benzyne has burgeoned since its derivatives were found to be responsible for the activity of the enediyne class of antitumor antibiotics,[8−11] the mechanism by which *para*-benzyne type intermediates damage DNA is not well understood.

* To whom correspondence should be addressed (e-mail: davidson@indiana.edu).

(1) (a) Sander, W. *Acc. Chem. Res.* **1999**, *32*, 669. (b) Nelson, E. D.; Artau, A.; Price, J. M.; Kenttämaa, H. I. *J. Am. Chem. Soc.* **2000**, *122*, 8781. (c) Thoen, K. K.; Kenttämaa, H. I. *J. Am. Chem. Soc.* **1999**, *121*, 800. Kraka, E.; Cremer, D.; Bucher, G.; Wandel, H.; Sander, W. *Chem. Phys. Lett.* **1997**, *268*, 313.

(2) Nicolaides, A.; Borden, W. T. *J. Am. Chem. Soc.* **1993**, *115*, 11951.

(3) (a) Wierschke, S. G.; Nash, J. J.; Squires, R. R. *J. Am. Chem. Soc.* **1993**, *115*, 11958. (b) Wenthold, P. G.; Squires, R. R. *J. Am. Chem. Soc.* **1994**, *116*, 6401.

(4) Lindh, R.; Lee, T. J.; Bernhardsson, A.; Persson, B. J.; Karlström, G. *J. Am. Chem. Soc.* **1995**, *117*, 7186.

(5) Kraka, E.; Cremer, D. *J. Am. Chem. Soc.* **1994**, *116*, 4929.

(6) Cramer, C. J.; Nash, J. J.; Squires, R. R. *Chem. Phys. Lett.* **1997**, *277*, 311.

(7) Lindh, R.; Bernhardsson, A.; Schütz, M. *J. Phys. Chem. A* **1999**, *103*, 9913.

(8) *Enediyne Antibiotics as Antitumor Agents*; Borders, D. B., Doyle, T. W., Eds.; Marcel Dekker: New York, 1995.

(9) (a) Kaneko, T.; Takahashi, M.; Hirama, M. *Tetrahedron Lett.* **1999**, *40*, 2015. (b) Jones, G. B.; Plourde, G. W., II; Wright, J. M. *Org. Lett.* **2000**, *2*, 811. (c) Dai, W.-M.; Fong, K. C.; Lau, C. W.; Zhou, L.; Hamaguchi, W.; Nishimoto, S. *J. Org. Chem.* **1999**, *64*, 682. (d) Konig, B.; Pitsch, W.; Thondorf, I. *J. Org. Chem.* **1996**, *61*, 4258. (e) Nicolaou, K. C.; Dai, W.-M.; Hong, Y.-P.; Tsay, S.-C.; Baldridge, K. K.; Seigel, J. S. *J. Am. Chem. Soc.* **1993**, *115*, 7944. (f) Nicolaou, K. C.; Liu, A.; Zeng, Z.; McComb, S. *J. Am. Chem. Soc.* **1992**, *114*, 9279. (g) Nicolaou, K. C.; Hong, Y.-P.; Torisawa, Y.; Tsay, S.-C.; Dai, W.-M. *J. Am. Chem. Soc.* **1991**, *113*, 9878. (h) Magnus, P.; Fortt, S.; Pitterna, T.; Snyder, J. P. *J. Am. Chem. Soc.* **1990**, *112*, 4986. (i) Nicolaou, K. C.; Owaga, Y.; Zuccarello, G.; Kataoka, H. *J. Am. Chem. Soc.* **1988**, *110*, 7247. (j) Magnus, P.; Carter, P. A. *J. Am. Chem. Soc.* **1988**, *110*, 1626.

(10) Konishi, M. *Antibiot.* **1989**, *42*, 1449.

(11) Smith, A. L.; Nicolaou, K. C. *J. Med. Chem.* **1996**, *39*, 2103. Kraka, E.; Cremer, D. *J. Am. Chem. Soc.* **2000**, *122*, 8245.

10.1021/ja0159620 CCC: $20.00
Published on Web 10/04/2001

Recently, Chen and co-workers[12] used the valence bond promotion energy (VBPE)[13−15] model to suggest that ΔE_{ST} may affect the rate of H-atom abstraction by *para*-benzyne, because this process involves partial uncoupling of the diradical electrons at the transition state (TS). These authors further speculated that triplet *para*-benzyne should abstract H-atoms at a rate similar to that for the phenyl radical. Because the singlet−triplet gap for *para*-benzyne is small (ΔE_{ST} = 4 kcal/mol),[16] the singlet radical pathway should be similar to, but slower than, that of phenyl radical.[17−19] The VBPE model may also be extended to the other benzyne isomers. For example, the large singlet−triplet gap in *ortho*-benzyne (ΔE_{ST} = 38 kcal/mol, respectively)[16] favors nucleophilic reactions over abstraction pathways.[20−23] The VBPE model also successfully predicts the trend in C−H bond dissociation energies for phenyl radical at the *ortho*-, *meta*-, and *para*- positions. Several authors have proposed that substituent effects may be used to control the magnitude of ΔE_{ST} in the benzyne diradicals, which in turn may alter their reactivity.[24−26]

Although many studies have focused on the geometry and electronic structure of the benzyne diradicals, to our knowledge, a systematic investigation of either H-atom addition or abstraction by both the singlet and triplet species has not been performed. Both of these pathways are important, depending on the distance of the H-atom donor to the radical centers of the benzyne. If the H-atom donor is far from the diradical, cleavage of the X−H bond will occur followed by H-atom addition to benzyne. However, if the H-atom donor is close to the radical center, an abstraction process is likely. In this work, we determine the ab initio potential energy surfaces (PESs) for the addition of H-atom to ground-state *ortho*-, *meta*-, and *para*-benzynes to yield the ground state of phenyl radical. To obtain greater insight, we also examine the ground-state singlet and first triplet states of H···H diradical undergoing H-atom addition and abstraction as a model for benzyne diradical reactions. Because molecular orbital methods delocalize the electrons in the system, valence bond (VB) techniques have been used to extract the contribution of "diradical" VB functions to the full configuration interaction (CI) wave function in the H_3 system. Our results indicate that mixing of the ground and first excited VB structures within the multiconfiguration wave function can be used to rationalize the unusual thermodynamics of H-atom addition to singlet and triplet benzynes. In sharp contrast to the addition process, the PES for H-atom abstraction in the singlet ground state is best described by the weakly avoided crossing of the dominant configurations in the CI wave functions of the S_0 and S_1 states. Consequently, the activation barrier for abstraction in the S_0 state will be largely unaffected by ΔE_{ST} of H···H diradical. A similar description may be applied to abstraction by triplet H···H.

Computational Methodology

Geometry optimizations of *ortho*-, *meta*-, and *para*-benzynes were performed with the complete active space self-consistent field (CASSCF) method and the 6-31G* basis set using the HONDO 99 program without any symmetry constraints.[27] In the first (larger) CAS, 8 electrons were distributed among 8 orbitals including the 3 out-of-plane π orbitals, the in-plane σ bonding and antibonding orbitals, and the 3 corresponding virtual π orbitals. The second (smaller) CAS was generated by distributing 2 electrons in only the σ bonding and antibonding orbitals of the radical centers. Subsequently, *m*-electron/*n*-orbital CASSCF calculations will be abbreviated (*m,n*)CASSCF.

The PESs for the addition of H-atom to the ground-state singlet benzynes were computed at the (9,9)CASSCF and (3,3)CASSCF levels. These wave functions were generated from the (8,8) and (2,2) CASs by including the antibonding C−H orbital in the active space. In each scan of the PES, the internal coordinates of the phenyl radical were frozen at the optimized CASSCF values, while the ortho, meta, or para C···H bond distance (r_{CH}) was altered.

The PES for addition of H-atom to H···H and the exchange reaction $H_2 + H{\cdots}H \rightarrow H^{\bullet} + H_2 + H^{\bullet}$ was performed at the full configuration interaction (CI) level with the same basis set. In the addition PES, all but one internal coordinate was frozen, while in the exchange reaction, the reactant H_2 internuclear distance was allowed to optimize at each point in the scan of S_0. Last, H-atom abstraction by H···H diradical from CH_4 was performed at the (4,4)CASSCF level with the same basis set using HONDO 99. The active space was composed of the bonding and antibonding C−H and H···H orbitals. In each scan of the PES (0.05 Å increments), the internal coordinates of CH_3 were frozen at the singlet B3LYP/6-31G* optimized geometry for CH_4, while the bond distance of the C···H of interest was allowed to optimize along the reaction coordinate.

H_3 Model of Benzyne H-Atom Addition

The reaction

$$H_A^{\bullet} + H_B{\cdots}H_C \rightarrow H_A{\cdots}H_B + H_C^{\bullet}$$

presents the simplest model of H-atom addition. When the $H_B{\cdots}H_C$ internuclear separation is much greater than the equilibrium bond length R_e (0.741 Å), the dihydrogen system may be thought of as a diradical. In this study, the PESs were determined for H-atom addition to the ground state of $H_B{\cdots}H_C$ at four r_{BC} distances: 1.00, 1.67, 2.00, and 3.00 Å. These systems represent H-atom addition to singlet diradicals that are strongly, moderately, and weakly stabilized relative to the first triplet state. Similarly, the PES for H-atom addition to the first triplet excited state of $H_B{\cdots}H_C$ was calculated as an approximation to H-atom addition to a triplet diradical.

The CI wave functions of H_3 along the reaction coordinate (Ψ_{CI}) were analyzed by resolving them into two distinct VB components (Ψ_{VB}) which describe the following doublet ($S = {}^1/_2$) spin couplings without ionic contributions:[28] either $^2[^2(H_A)^1(H_BH_C)]$ and $^2[^1(H_AH_B)^2(H_C)]$ or $^2[^2(H_A)^3(H_BH_C)]$ and $^2[^2(H_A)^1(H_BH_C)]$. The $^2[^3(H_AH_B)^2(H_C)]$ VB function was not used. The contribution of normalized Ψ_{VB} to Ψ_{CI} was estimated by the least squares weight, $w = \langle\Psi_{VB}|\Psi_{CI}\rangle^2$.

(12) Schottelius, M. J.; Chen, P. *J. Am. Chem. Soc.* **1996**, *118*, 4896.
(13) Clauberg, H.; Chen, P. *J. Am. Chem. Soc.* **1991**, *113*, 1445.
(14) Chen, P.; Clauberg, H.; Minsek, D. W. *J. Am. Chem. Soc.* **1992**, *114*, 99.
(15) Zhang, X.; Chen, P. *J. Am. Chem. Soc.* **1992**, *114*, 3147.
(16) Wenthold, P. G.; Squires, R. R.; Lineberger, W. C. *J. Am. Chem. Soc.* **1998**, *120*, 5279.
(17) Marquardt, R.; Balster, A.; Sander, W.; Kraka, E.; Cremer, D.; Radziszewiski, J. G. *Angew. Chem., Int. Ed.* **1998**, *37*, 955.
(18) Semmelhack, M. F.; Neu, T.; Foubelo, F. *Tetrahedron Lett.* **1992**, *33*, 3277.
(19) Grissom, J. W.; Gunawardena, G. U.; Klingberg, D.; Huang, D. *Tetrahedron* **1996**, *52*, 6453.
(20) Wittig, G. *Angew. Chem.* **1965**, *77*, 752.
(21) Brown, A. T.; Christopher, T. A.; Levin, R. H. *Tetrahedron Lett.* **1976**, *46*, 4111.
(22) Miller, R. G.; Stiles, M. *J. Am. Chem. Soc.* **1963**, *85*, 1798.
(23) Nunn, E. *Tetrahedron Lett.* **1976**, *46*, 4199.
(24) Johnson, W. T. G.; Cramer, C. J. *J. Am. Chem. Soc.* **2001**, *123*, 923.
(25) Cramer, C. J.; Debbert, S. *Chem. Phys. Lett.* **1998**, *287*, 320.
(26) Logan, C.; Chen, P. *J. Am. Chem. Soc.* **1996**, *118*, 2113.
(27) Dupuis, M.; Marquez, A.; Davidson, E. R. *HONDO 99.6*; IBM Corporation: Kingston, NY, 1999.
(28) Only two of the four VB functions are mutually independent. Thus, our approach examined two VB functions at a time. When Ψ_{VB}^{DS} and Ψ_{VB}^{DT} were used, they were symmetrically orthogonalized.

Scheme 1

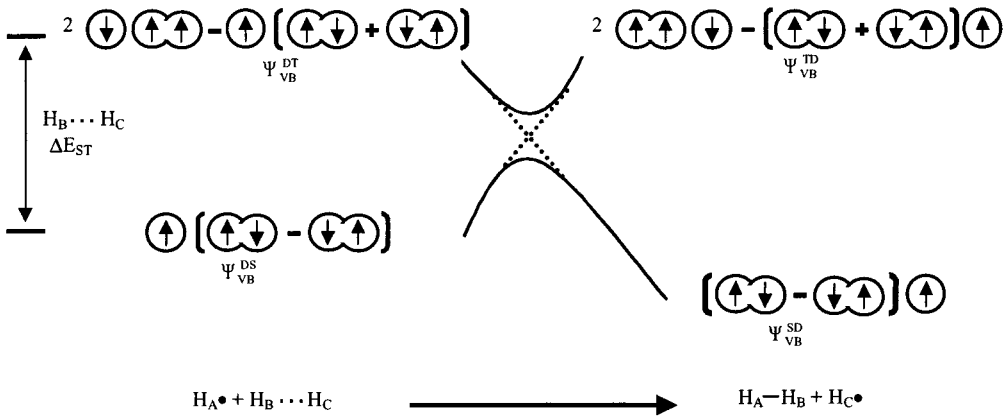

The particular unnormalized valence bond functions are given by

$$^2[^2(H_A)^1(H_BH_C)]: \quad \Psi_{VB}^{DS} = \left(\sqrt{\frac{1}{2}}\right)(\psi_1 - \psi_2)$$

$$[^2(H_A)^3(H_BH_C)]: \quad \Psi_{VB}^{DT} = \left(\sqrt{\frac{1}{6}}\right)(2\psi_3 - \psi_1 - \psi_2)$$

$$^2[^1(H_AH_B)^2(H_C)]: \quad \Psi_{VB}^{SD} = \left(\sqrt{\frac{1}{2}}\right)(\psi_2 - \psi_3)$$

$$^2[^3(H_AH_B)^2(H_C)]: \quad \Psi_{VB}^{TD} = \left(\sqrt{\frac{1}{6}}\right)(2\psi_1 - \psi_2 - \psi_3)$$

where ψ_1, ψ_2, and ψ_3 are Slater determinants:

$$\psi_1 = |\chi_A(\alpha),\chi_B(\alpha),\chi_C(\beta)|$$

$$\psi_2 = |\chi_A(\alpha),\chi_B(\beta),\chi_C(\alpha)|$$

$$\psi_3 = |\chi_A(\beta),\chi_B(\alpha),\chi_C(\alpha)|$$

and χ is the 1s atomic orbital of the isolated H-atom expanded in this basis set.

Similar to the qualitative VBPE approach, the H_3 model describes the effect of the first triplet state of the diradical on H-atom addition to a ground-state singlet. Although Chen's VBPE model was originally proposed specifically for H-atom abstraction by closed shell singlet species such as carbenes, it may be extended to addition processes by open shell diradicals such as benzyne. Correlation diagrams such as Scheme 1 illustrate the VBPE prediction that a ground-state singlet diradical must partially uncouple its radical electrons at the point of avoided crossing between the doublet ground state and first doublet excited state. The energetic gap associated with the addition TS is then directly related to the valence bond promotion energy, which is approximated by ΔE_{ST} of the $H_B \cdots H_C$ diradical.

In Scheme 1, the ground-state doublet (D_0) wave function of the H_3 reactant is represented by Ψ_{VB}^{DS}, while the corresponding excited state doublet (D_1) wave function is Ψ_{VB}^{DT}. Interestingly, the VB function of the addition product, Ψ_{VB}^{SD}, may be written as a linear combination of the initial D_0 and D_1 functions if atomic orbital overlap is neglected: $\Psi_{VB}^{SD} = -((\sqrt{3}/4)\Psi_{VB}^{DT} + (\sqrt{1}/4)\Psi_{VB}^{DS})$. The squares of the coefficients show that Ψ_{VB}^{SD} is 75% Ψ_{VB}^{DT} and 25% Ψ_{VB}^{DS}. Similarly, the D_1 state of the addition product (Ψ_{VB}^{TD}) is 25% Ψ_{VB}^{DT} and 75% Ψ_{VB}^{DS}. Although MO wave functions do not contain direct information about the interaction between VB states, VB contributions can be extracted from the CI wave function and used to better understand the influence of ΔE_{ST} on H-atom addition.

Table 1. ΔE_{ST} (kcal/mol) and N_D for Benzynes and Dihydrogen Diradicals Calculated by Various Methods and the 6-31G* Basis Set

	isomers		
	ortho	meta	para
N_D (2,2)CASSCF	0.77	1.38	1.94
ΔE_{ST} exptl[a]	37.5	21.0	3.8
ΔE_{ST} (8,8)CASSCF[b]	49.4	21.3	2.9
ΔE_{ST} (2,2)CASSCF[b]	41.8	17.5	0.9
	H···H model		
	1.67 Å	2.00 Å	3.00 Å
N_D full CI	0.94	1.40	1.96
ΔE_{ST} full CI	40.8	17.5	0.9

[a] See ref 16. [b] At the optimized singlet benzyne geometry.

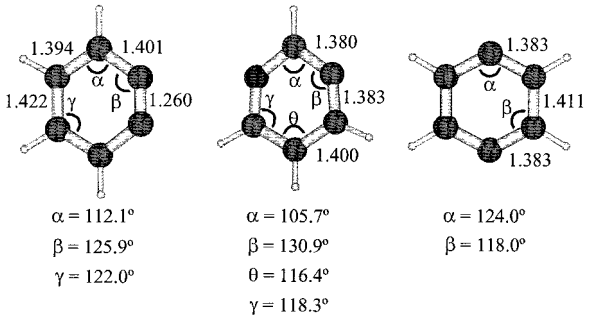

Figure 1. (8,8)CASSCF/6-31G* optimized geometries of *ortho*-, *meta*-, and *para*-benzyne in the ground state.

Results and Discussion

Benzyne Diradicals. The ground-state geometries and ΔE_{ST} values of the three benzyne isomers agree with previous studies (Table 1, Figure 1).[3] The optimized *ortho*- and *meta*-benzynes have C_{2v} structures, while *para*-benzyne has D_{2h} symmetry. The (8,8)CASSCF structures consistently have longer C−C bond lengths than those predicted by (2,2)CASSCF. These differences arise from excitations into the virtual π^* orbitals of the (8,8)-CAS. The π^* orbitals also facilitate "through-bond" interactions between the diradical electrons which increase the (8,8)CAS ΔE_{ST} values and decrease the inter-radical distances relative to the (2,2)CAS. The (8,8)CASSCF inter-radical distance in *ortho*-benzyne is 1.26 Å, which confirms that it is essentially a triple-

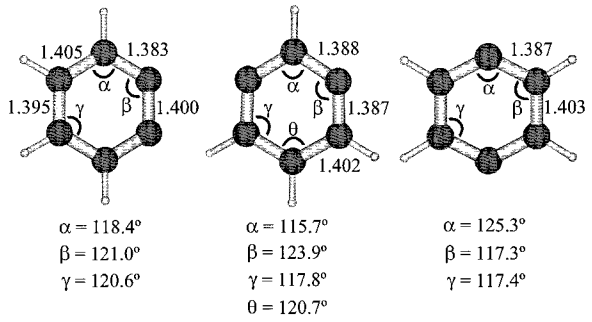

Figure 2. (8,8)CASSCF/6-31G* optimized geometries of *ortho*-, *meta*-, and *para*-benzyne in the first triplet excited state.

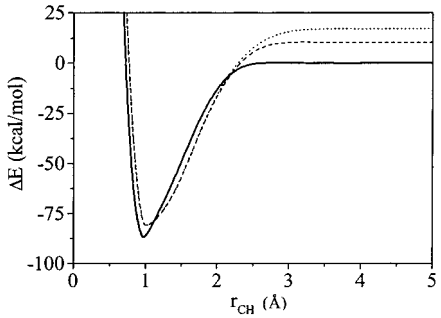

Figure 3. Relative ground state (9,9)CASSCF energy (kcal/mol) as a function of r_{CH} (Å), in the systems *ortho*-benzyne + H (solid line), *meta*-benzyne + H (dashed line), and *para*-benzyne + H (dotted line). The zero of energy is the sum of the energies of *ortho*-benzyne + H.

bonded species. This distance increases to 2.20 Å in *meta*-benzyne and reaches 2.71 Å in *para*-benzyne. The antisymmetric combination of in-plane p atomic orbitals in *para*-benzyne has some antibonding character from the σ^* orbital of the side bonds which increases the side bond lengths relative to those of the apical bonds.[29]

Previous studies have assessed the diradical character of the benzynes from a generalized VB wave function using the occupation numbers of the natural orbitals (NOs). We estimate the extent of diradical character of each benzyne by determining the number of effectively unpaired electrons, defined as $N_D = \int D(r)dr$, where $D(r)$ is the density of effectively unpaired (odd) electrons $D(r)$ introduced by Takatsuka et al[30,31] and N_D is related to the natural orbital occupation numbers, n_i, by the following equation:

$$N_D = \sum_{i=1}^{NO} n_i(2 - n_i)$$

At the optimized geometries, the N_D values obtained from the (2,2)CASSCF wave functions increase from 0.77 in *ortho*-benzyne to 1.38 in *meta*-benzyne and reach 1.94 in *para*-benzyne (Table 1). The same trend is observed when using the (8,8)CAS wave functions, but here, an additional 0.27 effectively unpaired electrons is associated with each π bond.

The geometries of the triplet benzynes differ noticeably from their singlet counterparts (Figure 2). The structure of each isomer in the triplet state is closer to that of benzene than in the singlet state. The (8,8)CASSCF inter-radical distances of *ortho*-, *meta*-, and *para*-benzyne increase to 1.40, 2.35, and 2.68 Å respectively. Interestingly, changes in bond length are the largest distortions in *ortho*- and *para*-benzyne, while *meta*-benzyne exhibits the largest distortions in bond angles. This indicates that the dominant interaction between the diradical electrons in singlet *ortho*- and *meta*-benzyne is through space, while the singlet diradical electrons in *para*-benzyne interact predominantly through other bonds. These interactions are further reflected in the order of the molecular orbitals in the CAS. In *ortho*- and *meta*-benzyne, through space interactions stabilize the bonding combination of in-plane p AOs relative to the antibonding combination. The opposite order is observed in *para*-benzyne, because the in-plane antibonding MO interacts with the σ^* orbital of the side bonds which stabilizes it relative to the bonding combination.

Dihydrogen Diradical. The H···H diradical effectively models the electronic properties of the benzynes when r_{BC} is chosen to produce the correct electronic coupling and diradical character. At r_{BC} = 1.00 Å, the ground-state singlet H···H diradical is more strongly coupled (ΔE_{ST} = 163 kcal/mol) and has less diradical character (N_D = 0.22) than any of the benzyne isomers (Table 1). However, we chose this model to represent the extreme case of coupling between diradical electrons that is similar to that of a molecule such as ethylene (ΔE_{ST} = 78 kcal/mol,[32] $N_D \approx 0.27$).[33] It will be interesting to compare this case to less coupled species such as the benzyne diradicals. An increase of r_{BC} to 1.67 Å decreases the electronic coupling to the levels suitable for modeling the ΔE_{ST} and N_D values of *ortho*-benzyne. The values of ΔE_{ST} = 41 kcal/mol and N_D = 0.94 computed with the (2,2)CASSCF in H_B···H_C (1.67 Å) are compared to values of 41 kcal/mol and 0.77 in *ortho*-benzyne, respectively. Similarly, at r_{BC} = 2.00 and 3.00 Å, ΔE_{ST} and N_D for dihydrogen are in good agreement with those for *meta*- and *para*-benzyne, respectively (Table 1).

D_0 PES for H-Atom Addition to Benzyne. Cuts through the (9,9)CASSCF PES for H-atom addition to the ground state of each benzyne isomer (at the fixed phenyl radical geometry) are shown in Figure 3. In agreement with the VBPE model, we observe that H-atom addition to *para*-benzyne is the most exothermic (ΔH_{298}= −97.2 kcal/mol), followed by *meta*- and *ortho*-benzyne (ΔH_{298}= −86.0 and −70.3 kcal/mol, respectively) (Table 2). The PES for *meta*- and *para*-benzyne merge at r_{CH} < 2.0 Å. Although the (3,3)CASSCF wave function is simpler, it produces almost the same results as the (9,9)CASSCF method. This result is important in light of the fact that the H_B···H_C model diradical only describes the σ framework of the benzyne. H-atom addition is slightly more exothermic in the (3,3)CASSCF because the calculated ΔE_{ST} decreases when the π space is neglected from the CAS.

D_0 PES for H-Atom Addition to H···H. The PESs of the H_3 model systems exhibit similar trends to those of the three benzyne isomers (Figure 4, Table 2). The PES for r_{BC} = 3.00 Å is the most exoenergetic (ΔE_0 = −95.7 kcal/mol), followed by r_{BC} = 2.00 Å (ΔE_0 = −83.7 kcal/mol), r_{BC} = 1.67 Å (ΔE_0 = −52.7 kcal/mol), and r_{BC} = 1.00 Å (ΔE_0 = −1.1 kcal/mol) (minimum energy of the r_{AB} structure relative to the full CI energy of H-atom plus H_B···H_C). Thus, the PES for H_3 with r_{BC} = 2.00 and 3.00 Å are in good agreement with *meta*- and *para*-benzyne, respectively, while r_{BC} = 1.67 Å PES has a similar shape to *ortho*-benzyne but only qualitatively correct energetics.

(29) Hoffmann, R.; Imamura, A.; Hehre, W. J. *J. Am. Chem. Soc.* **1968**, *90*, 1499.
(30) Takatsuka, K.; Fueno, T.; Yamaguchi, K. *Theor. Chim. Acta* **1978**, *48*, 175.
(31) Staroverov, V. N.; Davidson, E. R. *Chem. Phys. Lett.* **2000**, *330*, 161.
(32) *Excited States*; Lim, E. D., Ed.; Academic Press: New York, 1982; Vol. 5, pp 57−74.
(33) A value of 0.27 effectively unpaired electrons per π bond is typical.

Table 2. Thermodynamic Parameters (kcal/mol) for H-Atom Addition to Diradicals Computed with Various Methods and the 6-31G* Basis Set

	isomer		
	ortho	meta	para
D_0 ΔE_0 (9,9)CASSCF[a]	−89.4	−99.0	−105.7
D_0 ΔE_0 (3,3)CASSCF[a]	−93.7	−100.6	−107.5
D_0 ΔH_{298} (9,9)CASSCF[b]	−70.3	−86.0	−97.2
D_0 ΔH_{298} (3,3)CASSCF[b]	−75.9	−88.0	−98.6
	$H_A + H_B\cdots H_C$		
	r_{BC} 1.67 Å	r_{BC} 2.00 Å	r_{BC} 3.00 Å
D_0 ΔE_0[c] full CI	−52.7	−83.7	−95.7

[a] At the optimized phenyl radical geometry for both phenyl radical and benzyne without ZPE or thermal corrections [b] ZPE and thermal corrections included for enthalpy values using the optimized phenyl radical and benzyne structures [c] Energy of the optimized r_{AB} structure relative to the full CI energy of H-atom plus $H_B\cdots H_C$.

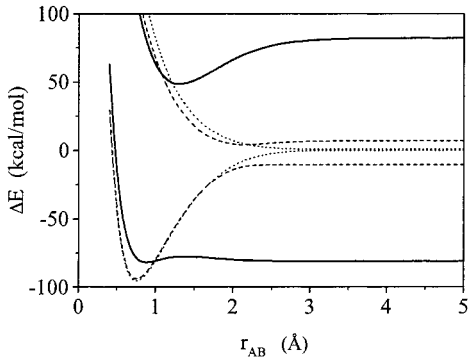

Figure 4. Relative ground and excited-state full CI energies (kcal/mol) of the $H_A\cdots H_B\cdots H_C$ system as a function of r_{AB} for $r_{BC} = 1.00$ Å (solid line), 2.00 Å (dashed line), and 3.00 Å (dotted line). For the purpose of clarity, the $r_{BC} = 1.67$ Å curve is not shown, and the energy of three H-atoms is taken to be zero.

Interestingly, the previous VBPE model predicts the existence of an activation barrier due solely to uncoupling of the diradical electrons to allow bond formation. Our results suggest that this barrier is present only in cases of extreme diradical coupling, such as in the H_3 model for $r_{BC} = 1.00$ Å ($\Delta E_0^{\ddagger} = 3.7$ kcal/mol). In these instances, the crossing of the dominant VB configurations in the D_0 and D_1 states will become more weakly avoided. Instead, the PESs for H-atom addition to benzyne diradicals and dihydrogen ($r_{BC} > 1.00$ Å) do not exhibit this phenomenon because of the strongly avoided crossing between these configurations in the D_0 and D_1 states. Because it is unlikely that substitution effects will drastically increase ΔE_{ST} of the benzyne diradicals, the TS energy for H-atom addition to benzynes should be minimally dependent on ΔE_{ST}.

VB Analysis of the PES for H_3. The shape of the PES for the H_3 models can be understood by examining the contribution of valence bond functions corresponding to $^2[^2(H_A)^1(H_BH_c)]$, $^2[^1(H_AH_B)^2(H_C)]$, and $^2[^2(H_A)^3(H_BH_C)]$ to the ground-state CI wave function of H_3 (Ψ_{CI}). When the H_A-atom is far from H_B (i.e., $r_{AB} \gg r_{BC}$), Ψ_{CI} of each H_3 model is composed mainly of the VB function that represents the singlet spin pairing of the diradical electrons (Ψ_{VB}^{DS}) on centers B and C. Conversely, when $r_{AB} < r_{BC}$, the electrons on centers A and B are paired in a singlet corresponding to the Ψ_{VB}^{SD} VB function (Figure 5).

In this instance, we use nonorthogonalized Ψ_{VB}, because Ψ_{VB}^{DS} and Ψ_{VB}^{SD} are not mutually exclusive even when the 1s overlap vanishes and their total contribution to Ψ_{CI} may be greater than unity. The H_3 model at $r_{BC} = 2.00$ Å is considered representative of all cases studied. The nonorthogonality between the two singlet VB functions increases dramatically at $r_{AB} < r_{BC}$.

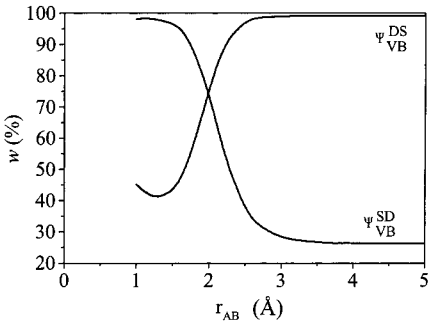

Figure 5. Contribution of nonorthogonalized VB functions Ψ_{VB}^{SD} and Ψ_{VB}^{DS} to Ψ_{CI} of the $r_{BC} = 2.00$ Å $H_B\cdots H_C$ model as a function of r_{AB}.

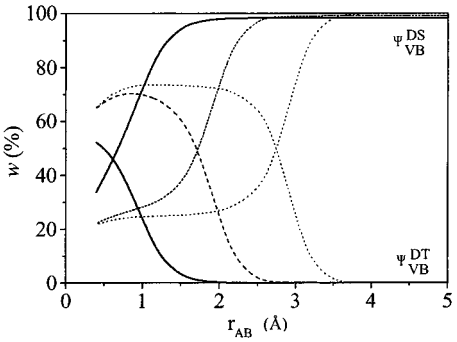

Figure 6. Contribution of symmetrically orthogonalized VB functions Ψ_{VB}^{DS} and Ψ_{VB}^{DT} to the ground-state CI wave function of H_3 as a function of r_{AB} at r_{BC} distances of 1.00 Å (solid line), 2.00 Å (dashed line), and 3.00 Å (dotted line). For the purpose of clarity, the $r_{BC} = 1.67$ Å data is not shown.

To understand the role of ΔE_{ST} on H-atom addition processes, it is important to decompose Ψ_{CI} into orthogonalized Ψ_{VB}^{DS} and Ψ_{VB}^{DT} components. As the H-atom approaches the radical center, the contribution of Ψ_{VB}^{DT} to Ψ_{CI} increases until the CI wave function is best represented as the VB function of the H-atom addition product (Ψ_{VB}^{SD}), which is approximately 75% Ψ_{VB}^{DT} and 25% Ψ_{VB}^{DS}. Indeed, the Ψ_{CI} of the addition product when $r_{BC} = 1.00$ Å is best described as 30% Ψ_{VB}^{DT} and 64% Ψ_{VB}^{DS} (Figure 6). At longer r_{BC}, the contributions of Ψ_{VB}^{DT} and Ψ_{VB}^{DS} approach the predicted values for Ψ_{CI} of the $H_A{-}H_B + H_C$ product. For example, at $r_{BC} = 3.00$ Å, Ψ_{CI} of the addition product is 71% of the initial Ψ_{VB}^{DT} and 24% of the initial Ψ_{VB}^{DS}. Similar results are obtained with $r_{BC} = 1.67$ and 2.00 Å. Interestingly, in each H_3 model, Ψ_{VB}^{DT} begins to contribute significantly to Ψ_{CI} in the vicinity of $r_{AB} \approx r_{BC}$. In this region, the interaction of the electrons on centers A and B becomes larger than the coupling between the $H_B\cdots H_C$ diradical electrons.

According to the VBPE model, decoupling of the diradical electrons is a necessary feature of H-atom addition to a singlet diradical. As we have just seen, a multiconfiguration wave function admixes the VB functions that correspond to triplet spin pairing of the diradical electrons into the ground-state wave function. The contribution of Ψ_{VB}^{DT} to Ψ_{CI} depends on the ΔE_{ST} of the isolated $H_B\cdots H_C$ diradical. When $r_{BC} = 1.00$ Å, the $H_B\cdots H_C$ diradical electrons are strongly coupled ($\Delta E_{ST} = 163$ kcal/mol) which hinders mixing of the Ψ_{VB}^{DT} and Ψ_{VB}^{DS} VB functions. The contribution of Ψ_{VB}^{DT} to Ψ_{CI} is greater when the system has a smaller ΔE_{ST}, such as when $r_{BC} = 1.67$, 2.00, and 3.00 Å. Similarly, the multiconfiguration wave functions of

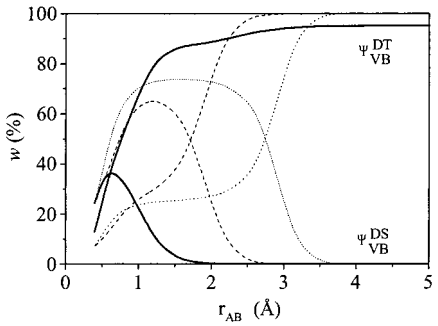

Figure 7. Contribution of orthogonalized Ψ_{VB}^{DS} and Ψ_{VB}^{DT} to the first excited-state CI wave function of H_3 as a function of r_{AB} at r_{BC} distances of 1.00 Å (solid line), 2.00 Å (dashed line), and 3.00 Å (dotted line).

benzyne + H should mix the "singlet" and "triplet" VB functions. The extent of mixing should follow the order *ortho-* < *meta-* < *para*-benzyne according to the trend in decreasing ΔE_{ST} with increasing distance between the radical centers. This not only leads to fast H-atom addition when ΔE_{ST} is small and slow rates when ΔE_{ST} is large, but it also correlates strongly with the observed C−H bond dissociation energies from phenyl radical at the ortho, meta, and para positions.

D_1 PES for H-Atom Addition to H···H. The calculation of the PES for H-atom addition to triplet benzyne is not straightforward. When the H-atom is far from a radical center, the lone electrons occupy the bonding and antibonding combinations of in-plane *p* orbitals $(\sigma)^1(\sigma^*)^1$. This region of the PES should be accurately described by the H_3 model system. However, when the interaction of the H-atom with the radical center becomes large, the dominant configuration in the CASSCF wave function becomes $(\pi)^1(\sigma^*)^1$, that is, the first doublet excited state of the phenyl radical abstraction product. The crossing between the $(\sigma)^1(\sigma^*)^1$ and $(\pi)^1(\sigma^*)^1$ states becomes avoided if the approaching H-atom is moved out of the plane and may give rise to a TS. The presence of such a TS would make it unlikely for H-atom abstraction to occur on this surface.

Unfortunately, calculations of the PES scan for H-atom addition by a triplet benzyne would not converge in the vicinity of the state crossing. Consequently, we treated the first doublet excited state of the H_3 model systems as an approximation to this region of the PES. The first quartet state might also be formed by the interaction of H-atom with triplet benzyne and could have been studied. However, it is almost certainly repulsive and was not examined. The PESs for H-atom addition to the $H_B\cdots H_C$ systems with various r_{BC} in the D_1 state are included in Figure 4. Addition to the triplet $H_B\cdots H_C$ diradical at $r_{BC} = 1.00$ Å is exoenergetic ($\Delta E_0 = -34$ kcal/mol), with a minimum at $r_{AB} = 1.2$ Å. However, for $r_{BC} = 1.67$, 2.00, and 3.00 Å, the PESs for H-atom addition are repulsive!

The PES for H-atom addition to the first excited state of dihydrogen may also be explained by examining the VB character of the CI wave function (Ψ_{CI}^*). When $r_{AB} \gg r_{BC}$, Ψ_{CI}^* is composed primarily of Ψ_{VB}^{DT}. The large ΔE_{ST} that occurs for $r_{BC} = 1.00$ Å again inhibits the contribution of alternative VB functions to the CI wave function. In this case, the contribution of Ψ_{VB}^{DS} is limited by large ΔE_{ST} values. As seen in Figure 7, the contribution of the "triplet" diradical VB function to Ψ_{CI}^* is consistently large along the reaction coordinate, though it does decrease from 95% for $r_{AB} \gg r_{BC}$[34] to 79% at the energy minimum. Conversely, the contribution of Ψ_{VB}^{DS} to Ψ_{CI}^* increases from zero to only 12% at $r_{AB} = 1.20$ Å. In addition, the total VB contribution to $\Psi_{CI}^*(\Psi_{VB}^{DT} + \Psi_{VB}^{DS})$ decreases from nearly 100% at the asymptotic limit to about 40% at the shortest r_{AB} distances. This indicates that, at short r_{AB}, these VB functions fail to adequately describe Ψ_{CI}^* because Rydberg type functions should be included in the VB description.

Similar to what is observed in the D_0 state of dihydrogen, the decreased ΔE_{ST} values of the $r_{BC} = 1.67$, 2.00, and 3.00 Å $H_B\cdots H_C$ diradicals lead to significant VB mixing in the CI wave function. The $H_B\cdots H_C$ models of *ortho-*, *meta-*, and *para*-benzyne are characterized by a large contribution of Ψ_{VB}^{DS} to Ψ_{CI}^*. The resulting PESs for H-atom addition are repulsive. As could be expected from the ΔE_{ST} values, the extent of VB mixing decreases with r_{BC}. For example, at $r_{AB} = 1.20$ Å and $r_{BC} = 3.00$ Å, Ψ_{CI}^* is 72% Ψ_{VB}^{DS} and 25% Ψ_{VB}^{DT}. Similarly, at the same r_{AB} but at $r_{BC} = 2.00$ Å, Ψ_{CI}^* is best described as 65% Ψ_{VB}^{DS} and 30% Ψ_{VB}^{DT}.

The results of the first excited-state H_3 PES indicate that H-atom addition to triplet benzynes may not be possible because of the increasing singlet coupling of the diradical electrons along the first portion of the reaction coordinate. Although counterintuitive at first, this conclusion follows from the VB analysis of the CI wave function. If one imagines that D_0 and D_1 are adequately described by Ψ_{VB}^{DS} and Ψ_{VB}^{DT}, then an increase in the contribution of Ψ_{VB}^{DT} in the ground state must increase the contribution of Ψ_{VB}^{DS} in the excited state, because the total contribution of Ψ_{VB}^{DS} and Ψ_{VB}^{DT} remains equal to 100%. Intersystem crossing (ISC) to the ground state may then be a competitive pathway along the first excited state, and the rate of ISC may determine the kinetics of the H-atom addition PES.

S_0 PES for H-atom Abstraction by H···H From H_2 and CH_4. A VB analysis of H-atom abstraction in a singlet state necessitates the use of two four electron configurations for the reactant and product states that utilize six Slater determinants. The particular unnormalized VB functions are given by

$$^1[^1(X{-}H_A)^1(H_BH_C)]: \quad {}^1\Psi_{VB}^{SS} = \left(\sqrt{\frac{1}{4}}\right)(\psi_4 - \psi_2 - \psi_6 + \psi_5)$$

$$^1[^3(X{-}H_A)^3(H_BH_C)]:$$

$$^1\Psi_{VB}^{TT} = \left(\sqrt{\frac{1}{12}}\right)(2\psi_1 - \psi_4 - \psi_2 - \psi_6 - \psi_5 + 2\psi_3)$$

$$^1[^2X^1(H_AH_B)^2(H_C)]: \quad {}^1\Psi_{VB}^{DSD} = \left(\sqrt{\frac{1}{4}}\right)(\psi_1 - \psi_4 - \psi_6 - \psi_3)$$

$$^1[^2X^3(H_AH_B)^2(H_C)]:$$

$$^1\Psi_{VB}^{DTD} = \left(\sqrt{\frac{1}{12}}\right)(2\psi_2 + 2\psi_6 + \psi_4 + \psi_5 - \psi_1 - \psi_3)$$

where ψ_1−ψ_6 are Slater determinants:

$$\psi_1 = |\chi_X(\alpha), \chi_A(\alpha), \chi_B(\beta), \chi_C(\beta)|$$

$$\psi_2 = |\chi_X(\alpha), \chi_A(\beta), \chi_B(\beta), \chi_C(\alpha)|$$

$$\psi_3 = |\chi_X(\beta), \chi_A(\beta), \chi_B(\alpha), \chi_C(\alpha)|$$

$$\psi_4 = |\chi_X(\alpha), \chi_A(\beta), \chi_B(\alpha), \chi_C(\beta)|$$

$$\psi_5 = |\chi_X(\beta), \chi_A(\alpha), \chi_B(\beta), \chi_C(\alpha)|$$

$$\psi_6 = |\chi_X(\beta), \chi_A(\alpha), \chi_B(\alpha), \chi_C(\beta)|$$

(34) In the asymptotic limit, Ψ_{VB}^{DT} only contributes 95% to Ψ_{CI}^* because of the significant amount of Rydberg character that is present in the $^3\Sigma_u^+$ state of H_2 at 1.0 Å internuclear separation.

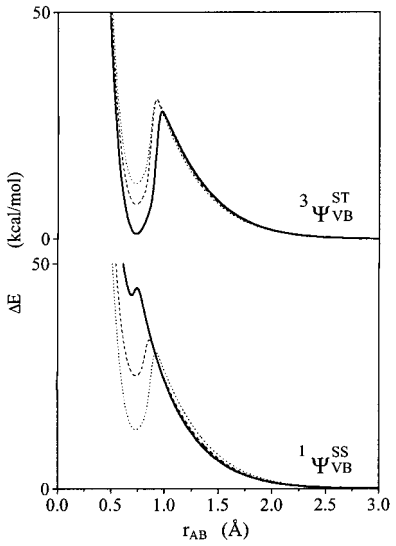

Figure 8. Relative (4,4)CASSCF/6-31G* energies (kcal/mol) of the PES for H-atom abstraction from CH_4 by singlet and triplet $H_B\cdots H_C$ as a function of r_{AB} for $r_{BC} = 1.67$ Å (solid line), 2.00 Å (dashed line), and 3.00 Å (dotted line). For the purpose of clarity, two energy scales are shown. In each PES, the energy of the curve at the asymptotic limit is taken to be zero.

In this case, the S_0 reactant VB configuration, $^1\Psi_{VB}^{SS}$, is formed from the singlet spin coupling of the X−H bonding electrons and those of the $H_B\cdots H_C$ diradical, while the first singlet excited-state configuration, $^1\Psi_{VB}^{TT}$, is formed from the combination of the excited triplet X−H bond and the triplet $H_B\cdots H_C$ diradical. Although the singlet−triplet energy gap is small for the $H_B\cdots H_C$ diradical, this gap is significant for the X−H bond, which leads to a very large energy difference between S_0 and S_1, ΔE_{SS}. This energy gap is still large when the H-atom abstraction product is examined. Similar to our analysis of the H-atom addition product, we find that the VB configuration of the S_0 H-atom abstraction product, $^1\Psi_{VB}^{DSD}$, may be written in terms of the reactant S_0 and S_1 VB functions if atomic orbital overlap is neglected: $^1\Psi_{VB}^{DSD} = -((\sqrt{3/4})^1\Psi_{VB}^{TT} + (\sqrt{1/4})^1\Psi_{VB}^{SS})$. Similarly, the S_1 VB function of the abstraction product is 25% $^1\Psi_{VB}^{TT}$ and 75% $^1\Psi_{VB}^{SS}$. Because the energy difference is initially large between the VB configurations of S_0 and S_1 along the abstraction reaction coordinate, a weakly avoided crossing is expected. Interestingly, previous VBPE discussions of H-atom abstraction by (σ,σ) diradicals such as singlet *para*-benzyne have acknowledged the triplet $H_B\cdots H_C$ diradical component to the $^1\Psi_{VB}^{DSD}$ VB configuration[12−14] while dismissing the triplet X−H character. Because the H-atom abstraction barrier in the S_0 state is dependent on ΔE_{SS}, which is itself mostly a function of the energy gap between the singlet and triplet X−H energies, the concept of adjusting diradical reactivity by altering ΔE_{ST} of $H_B\cdots H_C$ may need to be reconsidered.

Cuts of the PES for H-atom abstraction by the singlet state of the $r_{BC} = 1.67$, 2.00, and 3.00 Å separated $H_B\cdots H_C$ diradicals from CH_4 are presented in Figure 8. The activation barriers, $\Delta E_0^{\ddagger}$, for H-atom abstraction by the three diradicals are 42.2, 30.1, and 24.8 kcal/mol, respectively. Because the energy for changing the spin pairing of the X−H bond from singlet to triplet is the same for each curve, the differences in $\Delta E_0^{\ddagger}$ may be solely attributed to ΔE_{ST} of the $H_B\cdots H_C$ diradical. It is then readily apparent that ΔE_{ST} values that are greater than $\approx$ 30 kcal/mol are necessary to alter the relative strength of the avoided crossing of the $^1\Psi_{VB}^{SS}$ and $^1\Psi_{VB}^{TT}$ VB configurations, and thus $\Delta E_0^{\ddagger}$ in this example. In addition, the large ΔE_{SS} also makes the decomposition of the CI wave function into its VB components at each point along the PES unnecessary, because it will most likely resemble the results for the $r_{BC} = 1.00$ Å $H_B\cdots H_C$ model for H-atom addition. Namely, the VB configurations will not mix gradually along the reaction coordinate but will, instead, change very rapidly at the point of avoided crossing. Similar results were obtained for the exchange reaction of $H_B\cdots H_C$ with H_2 and are thus not presented.

Figure 8 also illustrates that, in this example, H-atom abstraction is endoenergetic because of the calculated relative bond energies of C−H versus H−H. Once again, however, the *para*-benzyne model exhibits the least endoenergetic PES ($\Delta E_0 = 11.0$ kcal/mol), followed by the *meta*-benzyne model ($\Delta E_0 = 23.0$ kcal/mol) and that for *ortho*-benzyne ($\Delta E_0 = 40.9$ kcal/mol). This is an indication of the effect of the $H_C^{\bullet}$ at a fixed distance from the abstraction product.

T_1 PES for H-Atom Abstraction by H···H from H_2 and CH_4. A four electron system may have three possible reactant triplet VB configurations and three product configurations that are composed from four Slater determinants. The VB configurations of interest in this study are given by

$$^3[^1(X{-}H_A)^3(H_BH_C)]: \quad ^3\Psi_{VB}^{ST} = \left(\sqrt{\frac{1}{2}}\right)(\psi_4 - \psi_3)$$

$$^3[^3(X{-}H_A)^1(H_BH_C)]: \quad ^3\Psi_{VB}^{TS} = \left(\sqrt{\frac{1}{2}}\right)(\psi_1 - \psi_2)$$

$$^3[^3(X{-}H_A)^3(H_BH_C)]: \quad ^3\Psi_{VB}^{TT} = \left(\sqrt{\frac{1}{4}}\right)(\psi_1 + \psi_2 - \psi_3 - \psi_4)$$

$$^3[^2X^1(H_AH_B)^2(H_C)]: \quad ^3\Psi_{VB}^{DSD} = \left(\sqrt{\frac{1}{2}}\right)(\psi_3 - \psi_2)$$

where $\psi_1-\psi_4$ are Slater determinants:

$$\psi_1 = |\chi_X(\alpha), \chi_A(\alpha), \chi_B(\alpha), \chi_C(\beta)|$$

$$\psi_2 = |\chi_X(\alpha), \chi_A(\alpha), \chi_B(\beta), \chi_C(\alpha)|$$

$$\psi_3 = |\chi_X(\alpha), \chi_A(\beta), \chi_B(\alpha), \chi_C(\alpha)|$$

$$\psi_4 = |\chi_X(\beta), \chi_A(\alpha), \chi_B(\alpha), \chi_C(\alpha)|$$

On the reactant side of the H-atom abstraction PES, the dominant VB configuration in the T_1 state is $^3\Psi_{VB}^{ST}$, which is formed from the singlet spin coupling of the X−H bonding electrons and the triplet pairing of the $H_B\cdots H_C$ diradical electrons. The next triplet state, T_2, may be written as the triplet coupling of the X−H electrons and the singlet pairing of the diradical, $^3\Psi_{VB}^{TS}$. T_3 is similar to S_1 in that it is formed from the triplet combination of both X−H and $H_B\cdots H_C$, $^3\Psi_{VB}^{TT}$. The T_1 product of the abstraction is degenerate with the S_0 state, because the singlet and triplet spin couplings of the separated doublet radical centers are nearly isoenergetic. Once again, the T_1 abstraction product may be written in terms of the reactant configuration such that $^3\Psi_{VB}^{DSD} = -(^1/_2{}^3\Psi_{VB}^{ST} + {}^1/_2{}^3\Psi_{VB}^{TS} + (\sqrt{1/2})\ ^3\Psi_{VB}^{TT})$. Thus, the T_1 abstraction PES should be characterized by an avoided crossing of VB configurations that is quite similar to the S_0 state. Indeed, cuts of the abstraction PES for $r_{BC} = 1.67$, 2.00, and 3.00 Å $H_B\cdots H_C$ diradicals (Figure 8) have $\Delta E_0^{\ddagger}$ values that are not only quite similar to one another ($\Delta E_0^{\ddagger} = 22.2$, 24.4, and 24.9 kcal/mol, respectively), but also to the S_0 activationbarriers. Interestingly, the ΔE_0 for the three

curves ($\Delta E_0 = -0.9$ kcal/mol, $\Delta E_0 = 5.6$ kcal/mol, and $\Delta E_0 = 10.0$ kcal/mol, respectively) are in the opposite order to that observed in S_0. This result is mostly due to the different relative energies of the three triplet $H_B\cdots H_C$ diradical reactants.

Conclusions

Use of the dihydrogen diradical is a simple and effective approach for studying (σ,σ) diradicals such as benzyne. The outcomes of both studies indicate that VB theory is a useful tool in understanding the reactivity of diradical systems, similar to previous VB studies of closed shell systems and S_N2 reactions.[35] The three and four electron model systems employed can only describe the σ framework of the benzyne diradicals, ignoring potential π effects on radical reactivity. However, because the general shape of the PES was not altered by including π orbitals in the CASSCF calculation for H-atom addition to benzyne, we feel that this is an adequate approximation.

The relative contributions of VB configurations to MCSCF wave functions along the H-atom addition PES are found not only to be dependent on the magnitude of ΔE_{ST} of the $H_B\cdots H_C$ diradical but also to change along the reaction coordinate. The ground-state reactant wave function is essentially the "singlet" VB configuration, $^2[^2(H_A)^1(H_BH_C)]$. However, as the H-atom approaches the radical center, the ground-state wave function gains significant "triplet" VB character which allows C−H bond formation. Conversely, the wave function of the D_1 state is predominantly the "triplet" VB configuration when the H-atom is far from a radical center but gains "singlet" VB character when the H-atom is close. As a result, the first excited addition PES is repulsive. Generally, if the contribution of the "triplet" VB configuration increases in the D_0 ground state, then the contribution of the "singlet" VB in the D_1 excited state has to increase, because the sum of contributions of the VB functions remains $\approx$ 100% along the reaction coordinate.

When applied to benzyne diradicals, the H_3 model accurately describes the observed order of exothermicity for ground-state H-atom addition: *ortho-* < *meta-* < *para*-benzyne. Interestingly, the avoided crossing between the "singlet" and "triplet" VB functions is so strong that an activation barrier associated with C−H bond formation is not observed. Furthermore, the H_3 model systems predict that VB mixing in the wave function will cause the PES for H-atom addition to triplet benzynes to be repulsive in the region where $r_{AB} < r_{BC}$. Any TS that is associated with the crossing or avoided crossing of the $(\sigma)^1(\sigma^*)^1$ configuration of the reactant and $(\pi)^1(\sigma^*)^1$ configuration of the phenyl radical along this surface may also depend on the amount of VB mixing in the $(\sigma)^1(\sigma^*)^1$ state which is a function of ΔE_{ST}.

The corresponding H-atom abstraction processes from both CH_4 and H_2 in both the singlet ground state and first triplet state are characterized by large activation barriers that result from the weakly avoided crossing of the dominant VB configurations in S_0 and S_1 and the three triplet states, respectively. Early in the reaction coordinate of the S_0 abstraction, the energy difference between S_0 and S_1 is very large, because the S_1 state is best described as the combination of the triplet X−H bond and the triplet $H_B\cdots H_C$. Because the S_0 abstraction product mostly derives from the S_1 reactant configuration, the activation barrier for abstraction is largely dependent on the singlet−triplet energy gap for the X−H bond instead of ΔE_{ST} of the $H_B\cdots H_C$ diradical. Thus, the concept of adjusting diradical reactivity by altering ΔE_{ST} of $H_B\cdots H_C$ may need to be reconsidered. Importantly, similar results are obtained for the T_1 state which indicate that the rate of H-atom abstraction should be similar to that of the ground-state singlet.

Acknowledgment. The authors wish to thank Viktor Staroverov and Professor Jeff Zaleski for thoughtful comments and the Graduate Assistance in Areas of National Need (GAANN) program administered by the Department of Education for a teaching/research assistantship. This work was supported by Grant CHE-9982415 from the National Science Foundation.

JA0159620

(35) Shaik, S. S. *J. Am. Chem. Soc.* **1981**, *103*, 3692. Shaik, S. S.; Pross, A. *J. Am. Chem. Soc.* **1982**, *104*, 2708. Pross, A.; Shaik, S. S. *J. Am. Chem. Soc.* **1982**, *104*, 187. Pross, A.; Shaik, S. S. *Acc. Chem. Res.* **1983**, *16*, 363.